ASSESSMENT OF A CURTAIN WALL SYSTEM USED IN HIGH-RISE BUILDINGS AND DEVELOPMENT OF A MONITORING METHOD

Shunsuke Toyao[1], Takuya Nagae[2], James Chen[3], Koichi Kajiwara[4], Yoshikazu Kanzaki[5], Yu-Lin Chung[6]

[1]NIKKEN SEKKEI LTD, Tokyo, Japan (Former student of Nagoya University Graduate School)
[2]Associate Professor, Disaster Mitigation Research Center, Nagoya University, Nagoya, Japan
[3]Researcher, National Cheng Kung University, Tainan, Taiwan (Former Researcher of Nagoya University)
[4]Director, Hyogo Earthquake Engineering Research Center (E-Defense), NIED, Hyogo, Japan
[5]FUJISASH LTD, Chiba, Japan
[6]Assistant Professor, National Cheng Kung University, Tainan, Taiwan
Email: nagae@nagoya-u.jp, kaji@bosai.go.jp, ylchung@mail.ncku.edu.tw

ABSTRACT

A metal curtain wall system was tested in the NCREE South Lab shaking table facility. Curtain walls have been designed in reference to the seismic design limit of a story drift angle of 1% in Japan. Such curtain wall system has a physical property to flexibly move together with seismic deformations of the main building frame. The mechanical connection of a fastener is designed to behave as a hinge. The flexibility of a curtain wall system can be utilized for the assessment of an entire building system. In this study, gyros showed a function to assess the movement of a curtain wall. A numerical model was developed representing the local deformations of a curtain wall.

Keywords: Shaking table test, metal curtain wall, numerical model, gyro, damage monitoring

INTRODUCTION

Immediately following earthquakes, the quick safety assessment of buildings is needed in order to make the right decisions concerning the evacuation of people inside buildings. Sequential earthquakes in many past events caused further casualties through the collapse of buildings which had cumulative damage. Assessment of safety or residual earthquake resistant capacity should be carried out as accurately as possible. Related damage monitoring methods for buildings have been developed with many kinds of technologies. This study focuses on the movement of the metal curtain wall generally used for office buildings. In Japan, curtain walls have been designed according to the demand value of an inter-story drift angle of 1%. Such curtain wall system is expected to flexibly move together with seismic deformations of the main building frame. First, a shaking table test was conducted in order to verify the stable seismic performance of a curtain wall system. Second, an applicability of gyro for curtain wall response assessment was verified including the integration technique of angular velocity. The test was conducted in the NCREE South Lab shaking table facility. Third, a numerical model was prepared in order to assess the movements of each component constituting the curtain wall system. This study considers the curtain wall monitoring technology combining the gyro sensor system and numerical analysis. Monitoring a curtain wall would be applicable to not only assessment of the curtain wall behavior itself, but also assessment of the main building frame behavior. The angle of the curtain wall frame is certainly related to the inter-story drift angle of the main frame, which is one of the most important engineering values in seismic design criteria.

TEST SPECIMEN

A two-story steel frame was used as the test frame accommodating the curtain wall system. Figure 1 shows the test steel frame set on the shaking table. The story height was 3.0 m, and span length 3.4 m.

The column bases were firmly fixed using high-tension bolts and very stiff base plates. A thick concrete slab was firmly fixed on the 2nd floor (2F) and the roof floor (RF). The test steel frame had a strength capacity to remain elastic when subjected to JMA Kobe 100% motion. JMA Kobe motion is one of the famous strong ground motions recorded in the 1995 Kobe earthquake. In the pretest using a white noise wave, the transfer function showed a first mode period of 0.25 sec.

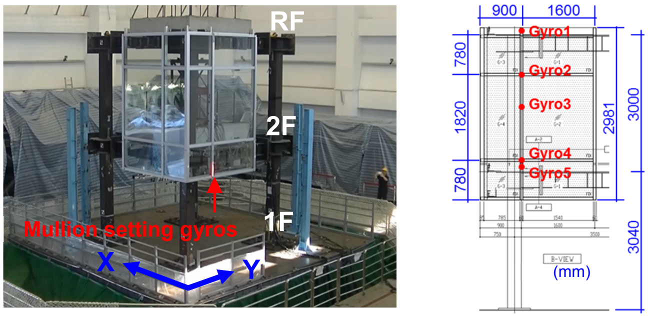

Figure 1. Test steel frame set on the shaking table and configuration of the test curtain wall

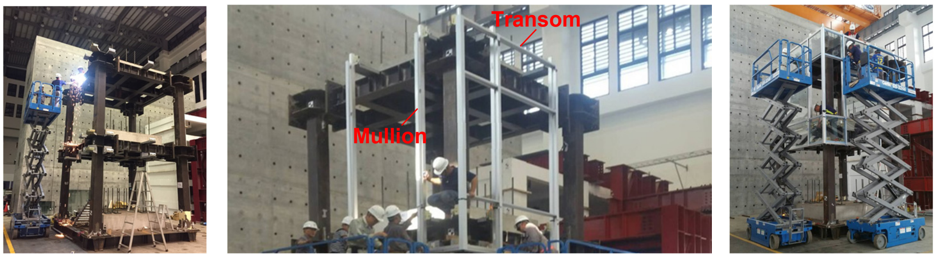

Figure 2. Installation process of a sash frame (mullion and transom) and glass panels

A general knock-down type of metal curtain wall was installed from the 2nd floor to the roof floor in the test steel frame. Figure 2 shows the installation process. The sash frame consisted of a mullion and transom. The transom was connected to the side of the mullion mechanically (mullion-transom connection). Four sizes of glass panel were used; height 1820 x width 1540, 780 x 1540, 1820 x 785, 780 x 785 (mm). The glass panel consisted of 2 glass plates with a thickness of 6 mm and a middle air layer with a thickness of 12 mm. The inter-drift level of this test was less than 0.5%. The clearance between the sash frame and glass panel was more than 7 mm. This value fulfills the design demand of 1%. Figure 3 shows the details of the fastener. The fasteners were fixed at the top of the beams of the roof floor and 2nd floor. In the lower part of the curtain wall, the specification of double fasteners, which is generally adopted at the bottom part of the lowest story of a building was adopted. For this reason, stiff lateral steel members were fixed at the bottom of the 2nd floor beam. Figure 4 shows photos of the installed fasteners and the lateral steel members. Silicone was used as the sealing material for gaps between the glass panel and sash frame.

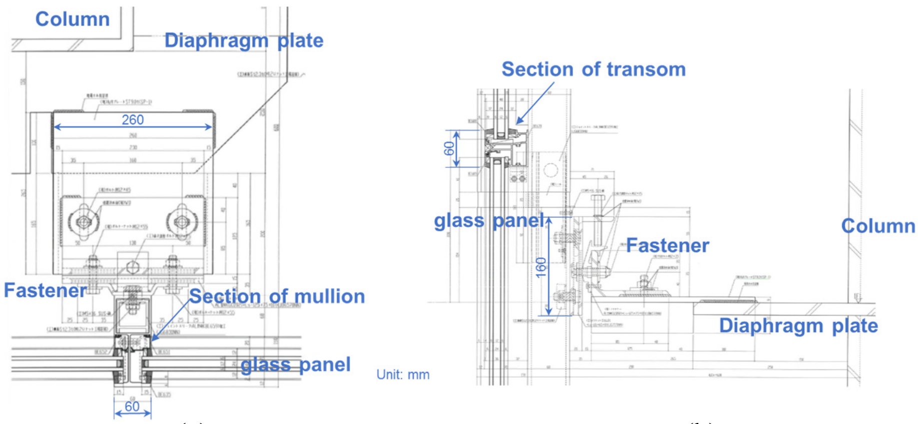

(a) (b)

Figure 3. Details of the fastener and sections of the mullion and transom:
(a) plan including section of mullion, (b) elevation including section of transom

Figure 4. Photos of fasteners fixed at the diaphragm plate or lateral steel member

TESTING PROTOCOL AND MEASUREMENT

The input motion to the shaking table was selected to represent the possible seismic response of a high-rise building. Figure 5 shows the concept. A 10-story reinforced concrete building frame was tested by using E-Defense in 2015. The frame exhibited inelastic behaviors in the JMA Kobe 100% motion with a dominant period of 1.0 sec. The response acceleration time histories of 3 directions are available for each floor, and the 7th floor records were adopted. As a result, full 3-directional shaking was realized with the capacity of the NCREE South Lab shaking table facility.

Figure 5. Shaking table input motion taken from a past E-Defense test (10-story frame, 2015)

Accelerometers were placed on the shaking table, 2nd floor and roof floor. The displacements were measured by the motion capture system. Targets for the motion capture system were placed on the shaking table, 2nd floor and roof floor. The mullion measured by gyros is shown in Figure 1. The number of used gyros was 5. Each height level is shown in Figure 1. These heights were selected for the estimation of displacement distribution. Figure 6 shows the specification of gyro. The Gyro attached on the mullion is also shown. Gyro 2 and Gyro 4 were located at the heights of the connections of the mullion and transom. Gyro 1 and Gyro 4 were located at the heights of fasteners. Gyro 3 was located at the intermediate height of the 2nd story. As for the horizontal displacements of the mullion, the in-plane direction was assessed. Thus, angular velocity of the gyro was recorded in the corresponding degree of freedom shown in the photo. The story drift angle of Y-direction was used for comparison.

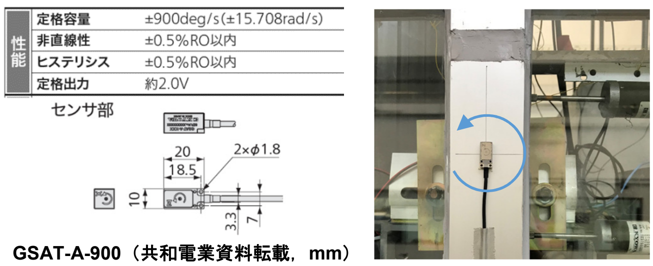

Figure 6. Specification of gyro attached to the mullion

TEST RESULT

In the test, the target floor response was reproduced accurately. The maximum displacement of Y direction was 406 mm at the shaking table and 424 mm at the roof floor of the test frame. The maximum velocity of Y direction was 1.54 m/s at the shaking table and 1.89 m/s at the roof floor of the test frame. The maximum acceleration of Y direction was 1.29 g at the shaking table and 2.12 g at the roof floor of the test frame. The maximum inter-story drift angle was slightly less than 0.5%. After the test, no damage was observed at the mullion-transom connections or fasteners.

Figure 7 shows the angular velocity time history recorded by the gyro and its Fourier spectrum. The dominant frequency of 1 Hz of the spectrum is consistent with the dominant frequency of input motion. Figure 8 shows the estimation process of gyro data. A Bandpass filter of 0.5-50 Hz was applied when integrating the angular velocity time history. The time history of the calculated angle was stable. Thus, the gyro-estimation angles at different heights were obtained by Gyro 1- Gyro 5.

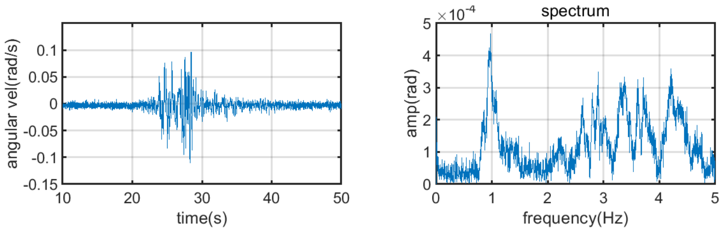

Figure 7. Angular velocity time history and its Fourier spectrum

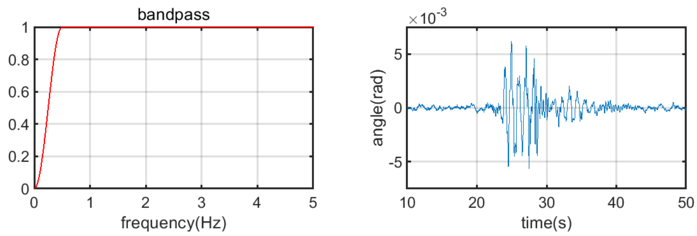

Figure 8. Bandpass filter and gyro-estimation angle time history

Figure 9 shows the time histories of inter-story drift angle and gyro-estimation angle. From the beginning to the end, the time histories of inter-story drift and gyro-estimation angles show waves with the same phase, indicating that the mullion flexibly tilted together with the relative displacement between the 2nd floor and roof floor. The lower figure in Figure 9 focused on the main time duration, which is between 10 sec and 17 sec. The figure shows clear differences of the maximum amplitude in gyro-estimation angles and inter-story drift at each peak. In the lower figure of Figure 9, the angle of

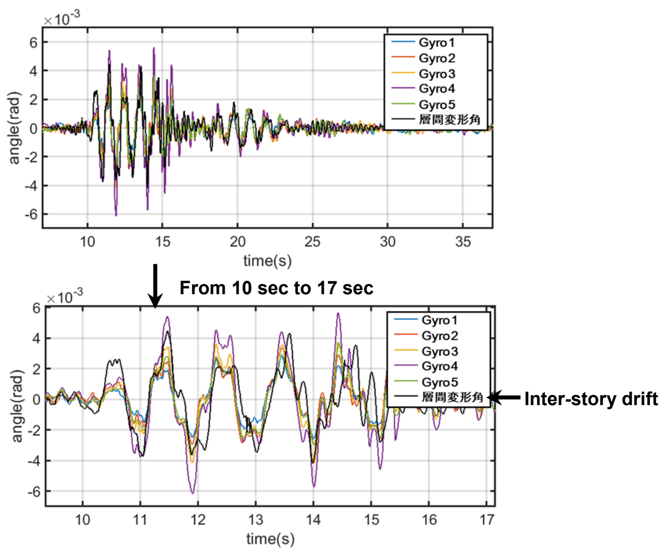

Figure 9. Time histories of angles and inter-story drift

Gyro 1, the blue line, shows the smallest values at every peak, and the angle of Gyro 4, the purple line, shows the largest values at every peak. The angle of Gyro 3 located at the intermediate height of the story, yellow line, shows the closest values to inter-story drift angle. Double fasteners fixed at the top and bottom of the 2nd floor beam create bending resistance at the lower part of the mullion. Such boundary condition had a significant impact on the displacement distribution of the mullion. Meanwhile, the mullion-transom connections had rotational deformations. The sash frame and glass panel had relative displacements causing shear deformation in the sealing material. These interactions eventually cause damage to the curtain wall in the larger deformation range (Nagae et al. 2008; Yamada et al., 2008; Nagae et al., 2010).

The displacement distributions of the mullion are assessed at selected peaks. The peaks of *i*-th (*i*=1-5) are shown in Figure 10 (a). The relative horizontal displacements of the mullion were zero at the heights of fasteners fixed at the top and bottom of the 2nd floor beam. Five gyros were set on the mullion. Here, the displacement distributions between the 2nd floor and roof floor are defined by 7th-degree polynomials. The origin of the distribution function is the height of the 2nd floor. The relative displacement of the roof floor is known as measured in the test. By the 8 condition functions shown in Figure 10 (b), the 7th-degree polynomial is defined; the coefficients, *a, b, c, d, e, f, g, h* are calculated at each peak (*i*=1-5), and the polynomials represent the displacement distributions of the mullion at each peak (*i*=1-5). Figure 10 (c) shows the results of calculation. If the mullion has no curvature, the displacement distribution line is straight and can be identical to the dotted line of the inter-story drift angle.

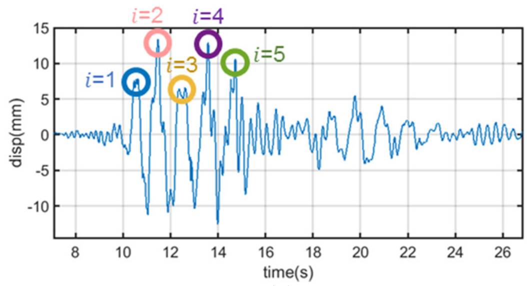

(a)

$$f_i(y) = ay^7 + by^6 + cy^5 + dy^4 + ey^3 + fy^2 + gy + h$$

$$\begin{cases} f_i'(y_1) = \theta_1 & \cdots \text{ Integrated value of Gyro 1} \\ f_i'(y_2) = \theta_2 & \cdots \text{ Integrated value of Gyro 2} \\ f_i'(y_3) = \theta_3 & \cdots \text{ Integrated value of Gyro 3} \\ f_i'(y_4) = \theta_4 & \cdots \text{ Integrated value of Gyro 4} \\ f_i'(y_5) = \theta_5 & \cdots \text{ Integrated value of Gyro 5} \\ f_i(y_1) = d_{RF} & \cdots \text{ Relative lateral displacement (RF-2F)} \\ f_i(y_5) = 0 & \cdots \text{ Fastener position Fixed at 2F beam} \\ f_i(y_6) = 0 & \cdots \text{ Fastener position Fixed at 2F beam} \end{cases}$$

(b)

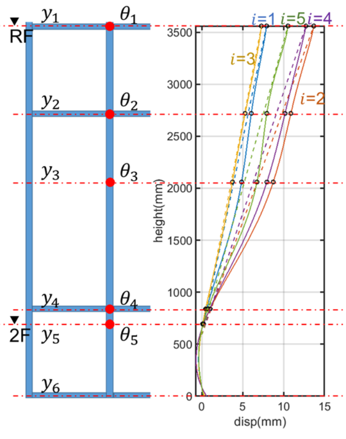

(c)

Figure 10. Assessment of test responses: (a) peaks of the inter-story drift time history, (b) displacement distribution function expressed by the 7th-degree polynomial, (c) displacement distribution function (solid line) and inter-story drift line (dotted line) at *i*-th peak

NUMERICAL MODEL

Figure 11 shows the configuration of the numerical model. The components of the curtain wall were modeled for (1) sash frame consisting of mullion and transom, (2) glass panel, (3) fastener connecting mullion and test frame, (4) sealing material between the sash frame and glass panel.

Figure 12 shows the modeling methods of interaction between the sash frame and glass panel. The presence of sealing material was reflected in the modeling. For the sash frame, the mullion and transom were modeled by elastic beam elements. The sections of mullion and transom have a hollow space, and the section shapes are complex. The moment of inertia was estimated by a calculation function prepared in Auto Cad. Young's modulus of the sash frame was defined by a nominal value of aluminum. Glass panels were modeled using 4 firmly connected rigid beams. The connection of the mullion and transom was modeled using a rotational spring. The fastener was modeled by the rotational spring. The sealing material was modeled by 1-D springs in reference to the size of gap between the sash frame and glass

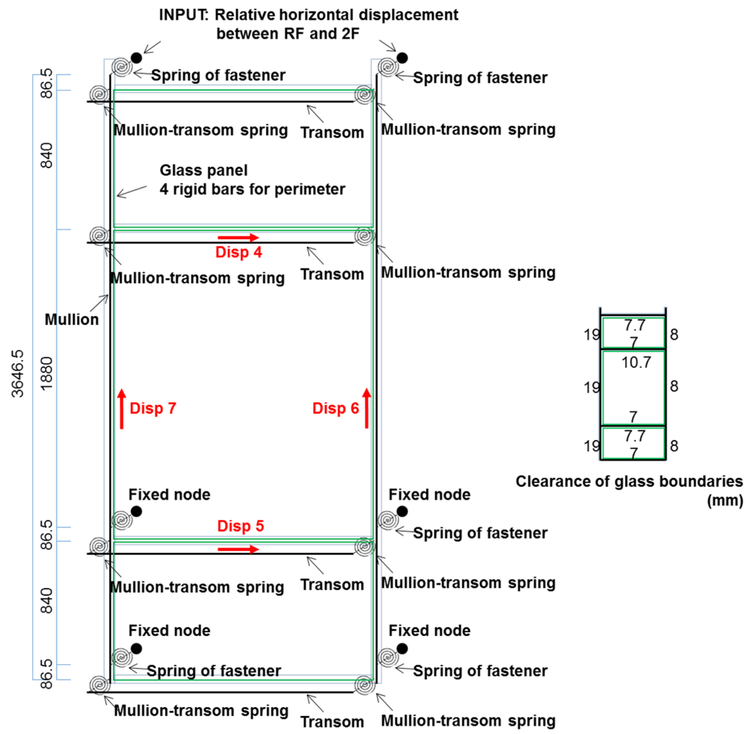

Figure 11. Configuration of numerical model for curtain wall (Unit: mm)

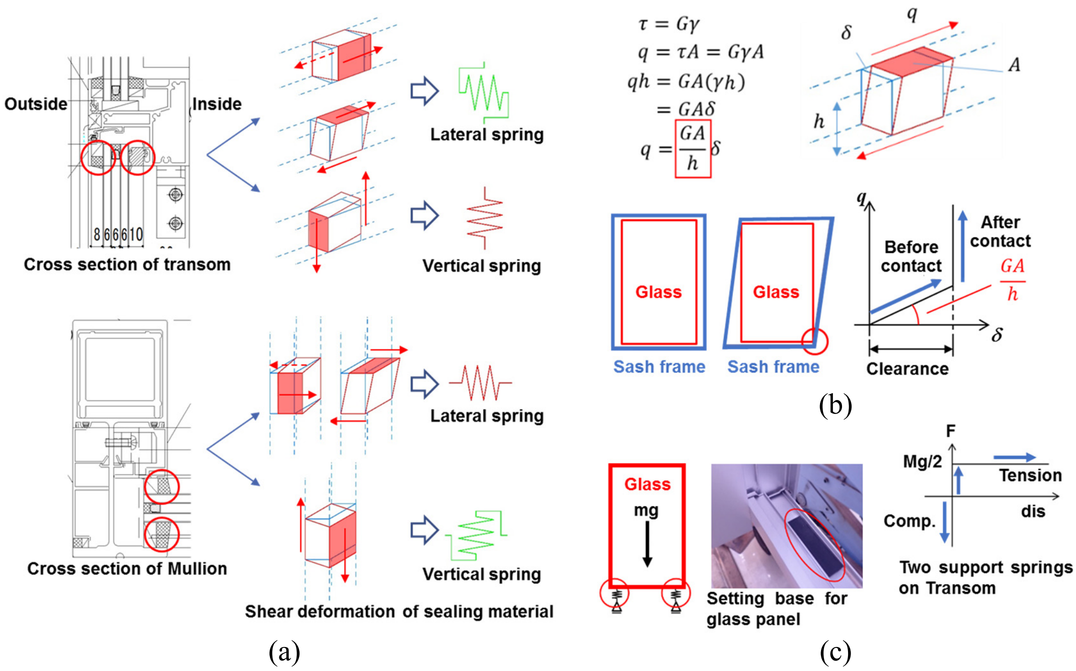

Figure 12. Sash frame - glass panel interaction modeling: (a), (b) 1-D spring property of sealing material, (c) 1-D spring property at the location of two setting bases beneath a glass panel

panel as well as the shear stiffness of silicone. The glass panel starts rocking when the edge of the panel makes contact with the edge of the sash frame. Uplifting of the glass panel is related to the weight of the glass panel and setting base locations. Such mechanism was incorporated using the equivalent vertical and lateral 1-D springs shown in Figure 12 (b) (c). However, the deformation level of the test steel frame was much smaller than the contacting deformation of the glass panel and sash frame. This aspect of the numerical model will be verified in reference to the past test data (Nagae et al. 2008; Yamada et al., 2008; Nagae et al., 2010).

Figure 13 shows the displacement distribution of gyro estimation as the test result (solid line), and also shows the displacement distribution given by numerical analysis (sequential plots). Both displacements of the test result and numerical analysis are zero at the fastener locations of the 2nd floor. Because the numerical analysis is inputting the relative displacements of the test result at the roof floor, both values of the test result and numerical analysis are identical. In Case 1, the rotational springs of fasteners are “pin”, and the rotational springs of mullion-transom connections are also “pin”. Here, “pin” means a rotational stiffness of zero. The displacement distributions of numerical analysis are curved to swell inward (leftward) while those of the test result are curved to swell outward (rightward). In Case 2, the rotational springs of fasteners are “pin” while the rotational springs of the mullion-transom connections have the rotational stiffness of theoretical value (Appendix: K=2.5 x 10^{11} Nm/rad). Both curves of the test result and numerical analysis swell outward. In Case 3, the rotational springs of the upper part have a relatively large rotational stiffness while the rotational springs of the lower part have a relatively small rotational stiffness. The curves of numerical analysis match those of the test result by tuning the rotational stiffness distribution. The presence of a glass panel had negligible impact on the displacement distribution in the numerical analysis. Figure 14 shows the relative displacements between

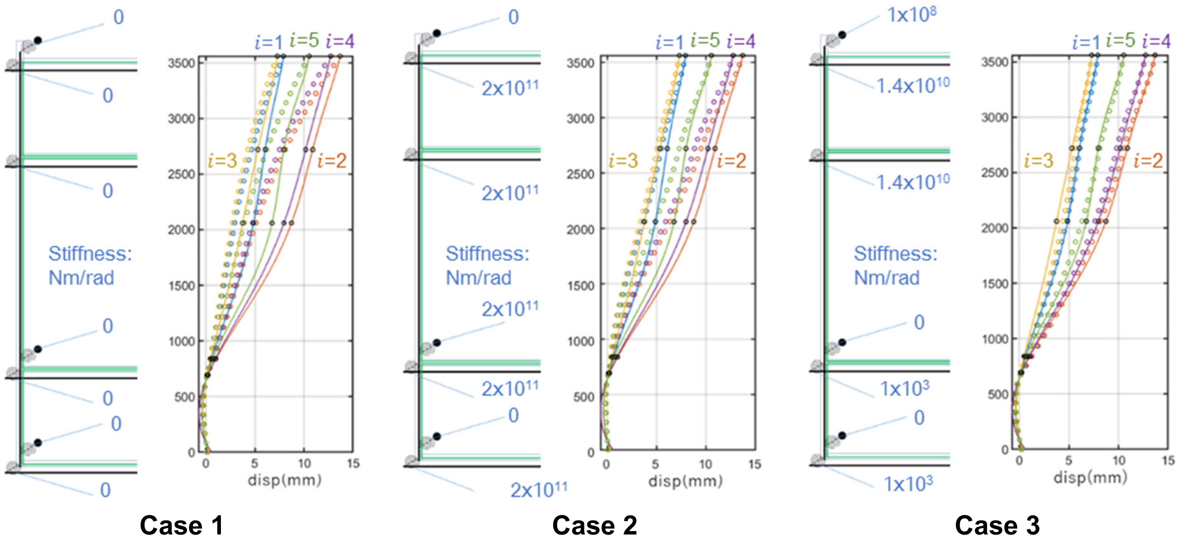

Figure 13. Displacement distributions of the test result (solid line) and numerical analysis (plots)

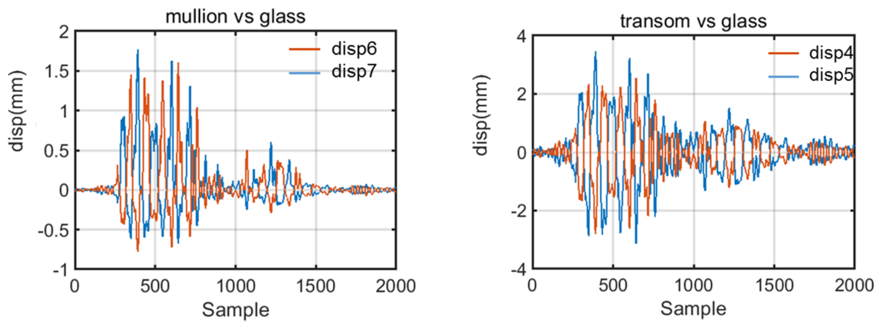

(a) (b)

Figure 14. Relative displacement between the sash frame and glass panel:
(a) mullion v.s. glass panel, (b) transom v.s. glass panel

sash frame and glass panel. The measuring positions of Disp 4-7 are shown in red in Figure 11. These relative displacement aspects can be utilized to assess the damage state of a curtain wall.

CONCLUSIONS

A metal curtain wall system was tested in the NCREE South Lab shaking table facility in September 2018 A knock-down type of curtain wall was installed in a test steel frame. The curtain wall was designed according to the design demand of a story drift angle of 1%. The sash frame consisted of a mullion and transom. The fastener had a mechanical hinge connection. Glass panels were installed in the sash frame, and their gaps were sealed by silicone. The curtain wall system showed its physical property to flexibly move together with the deformations of the test steel frame. A numerical model was developed to represent the movements of each component constituting the curtain wall system. The displacement distribution of the mullion was estimated by using gyro. The angular velocity given by gyro was appropriately integrated, and the angles were calculated at 5 heights of the mullion providing the displacement distribution function. The numerical model has to be revised to trace the displacement distributions observed in the test. Efficient procedures can be developed by accumulating additional test data and verifications. The curtain wall monitoring procedure combining gyro instrumentation assessment and numerical analysis may be a promising option. Curtain wall monitoring methods and other existing monitoring methods can be integrated. This would significantly contribute to the comprehensive damage monitoring methodology for an entire building system.

ACKNOWLEDGMENTS

The authors greatly appreciate the advice and support of Professor George-C. Yao of NCKU. The authors are deeply grateful for the strong technical support of the technicians of the NCREE South Lab facility. From Japan, Mr. Hiratsuka, Mr. Fukui and Mr. Ohta of FUJISASH LTD fully prepared the test curtain wall as well as its instrumentation.

APPENDIX

The first-order differentiation of the displacement distribution function given in Figure 10 (c) is the distribution function of the rotation angle. The second-order differentiation of the displacement distribution function is the distribution function of curvature. The moment distribution function of the mullion is given by a product of the curvature, the moment of inertia of the section area and Young's modulus of aluminum. The moment shown at the height of the mullion-transom connection was almost linearly related to the measured rotation angle of the connection. The rotational stiffness of the connection was estimated as 2.5 x 10^{11} (Nm/rad) in reference to the gradient.

REFERENCES

Takuya Nagae, Kouich Kajiwara, Hideo Fujitani, Kunio Fukuyama, Hidenori Kawabe, Masayoshi Nakashima (2008). "Behaviors of Nonstructural Components in Seismic Responses of High-Rise Buildings/E-Defense Shaking Table Test" *14th World Conference in Earthquake Engineering*, 14_S10-010.

K. Yamada, H. Fujitani, H. Sakae, S. Yasuda, T. Nagae, K. Fukuyama, K. Kajiwara, Y. Kanno, H. Kawabe, S. Kido, and M. Nakashima (2008). "Behavior of Exterior Curtain Wall of High-Rise Buildings against Large Story Drift by Long-Period Earthquake Ground Motions" *14th World Conference in Earthquake Engineering*, 14_S10-040.

Takuya Nagae, Hideo Fujitani, Kunio Fukuyama, Shiro Kido (2010). "Performance of An Exterior Metal Curtain Wall in Seismic Responses of A High-Rise Building －E-Defense shaking table tests－" *The AIJ Journal of Technology and Design*, Vol. 16, No. 33, 535-540, June 2010 (in Japanese)